Phase Behavior of Polyion−Surfactant Ion Complex Salts: Effects of Surfactant Chain Length and Polyion Length

Anna Svensson, Jens Norrman, and Lennart Piculell*

Division of Physical Chemistry 1, Center for Chemistry and Chemical Engineering, Lund University, P.O. Box 124, SE-221 00 Lund, Sweden

Received: December 20, 2005; In Final Form: March 30, 2006

The aqueous phase behavior of a series of complex salts, containing cationic surfactants with polymeric counterions, has been investigated by visual inspection and small-angle X-ray scattering (SAXS). The salts were alkyltrimethylammonium polyacrylates, C_xTAPA_y, based on all combinations of five surfactant chain lengths (C_6, C_8, C_{10}, C_{12}, and C_{16}) and two lengths of the polyacrylate chain (30 and 6 000 repeating units). At low water contents, all complex salts except C_6TAPA_{6000} formed hexagonal and/or cubic *Pm*3*n* phases, with the hexagonal phase being favored by lower water contents. The aggregate dimensions in the liquid crystalline phases changed with the surfactant chain length. The determined micellar aggregation numbers of the cubic phases indicated that the micelles were only slightly aspherical. At high water contents, the C_6TAPA_y salts were miscible with water, whereas the other complex salts featured wide miscibility gaps with a concentrated phase in equilibrium with a (sometimes very) dilute aqueous solution. Thus, the attraction between oppositely charged surfactant aggregates and polyions decreases with decreasing surfactant chain length, and with decreasing polyion length, resulting in an increased miscibility with water. The complex salt with the longest surfactant chains and polyions gave the widest miscibility gap, with a concentrated hexagonal phase in equilibrium with almost pure water. A decrease in the attraction led to cubic−micellar and micellar−micellar coexistence in the miscibility gap and to an increasing concentration of the complex salt in the dilute phase. For each polyion length, the mixtures for the various surfactant chain lengths were found to conform to a global phase diagram, where the surfactant chain length played the role of an interaction parameter.

Introduction

Aqueous mixtures of oppositely charged polymers and surfactants have been extensively studied during several decades.[1−3] An associative phase separation readily occurs in the mixtures, due to the strong electrostatic attraction between the polyion and the oppositely charged surfactant aggregate. The associative phase separation results in one or more concentrated phase(s), enriched in the polyions and the surfactant, in equilibrium with a dilute phase containing most of the simple counterions.[3−5]

In recent years, an increasing interest has been directed to the concentrated phases and the parameters that control their appearance.[6−12] Macroscopically, a concentrated phase may be solidlike or liquidlike, depending on factors such as the polyion/surfactant ratio and on the total amount of salt in the system. Sometimes a solidlike phase contains highly ordered structures of surfactant aggregates with polyions as counterions.

Conventional mixtures of polyelectrolytes and oppositely charged surfactants are four-component systems (water + four ions, where the contents of the ionic components are restricted by electroneutrality). To obtain a better understanding of the factors controlling the phase separation, we recently introduced a new, simplifying approach to the study of oppositely charged polymer−surfactant mixtures,[13,14] where we used the *polyion−surfactant ion complex salt* as our point of departure; see Figure 1. The complex salt contains only surfactant ions and polyions

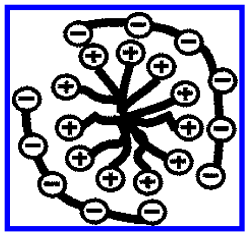

Figure 1. Polyion−surfactant ion complex salt contains one surfactant ion per polyion charge and no other ions.

and represents the energetically most preferred pairing of the ions in the mixture. By mixing the complex salt with either the surfactant or the polyelectrolyte in water, we obtain truly ternary systems (three ions + water), that is, mixtures with a reduced number of ions compared with the conventional mixtures.

In previous studies, we made extensive investigations of aqueous mixtures based on the complex salt cetyltrimethylammoniumpolyacrylate, where we used a short polyacrylate polyion (30 repeating units).[13,14] We will refer to this complex salt as $C_{16}TAPA_{30}$. Phase diagrams obtained in these studies for mixtures of $C_{16}TAPA_{30}$ with the surfactant $C_{16}TAAc$ or with the polyelectrolyte $NaPA_{30}$ are reproduced in Figure 2. Together, these phase diagrams describe a pathway where the polyion/surfactant ion ratio is changed continuously, from a surfactant-free polyelectrolyte solution to a polyion-free surfactant solution, in mixtures containing the minimum number of components. Interestingly, we see that the phase structures observed for aqueous $C_{16}TAAc$, that is, the micellar, cubic, and hexagonal phases, appear over most of the mixing ratios. We also see that

* To whom correspondence should be addressed. E-mail: lennart.piculell@fkem1.lu.se. Fax: +46 46 222 44 13.

10.1021/jp057402j CCC: $33.50
Published on Web 05/06/2006

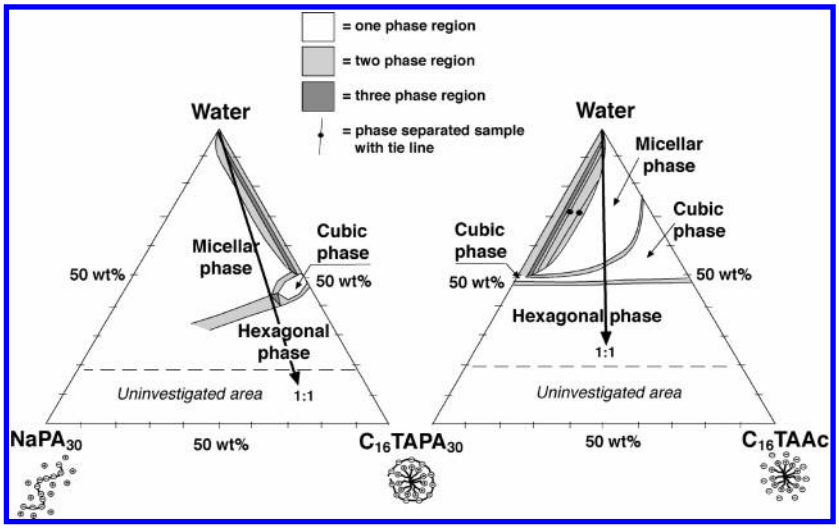

Figure 2. Experimental phase diagrams[14] at 25 °C of (a) (left triangle) the complex salt $C_{16}TAPA_{30}$, the polyelectrolyte $NaPA_{30}$, and water and (b) (right triangle) the complex salt $C_{16}TAPA_{30}$, the surfactant $C_{16}TAAc$, and water.

the liquid crystalline phases are continuous, that is, all cubic (hexagonal) samples belong to the same cubic (hexagonal) phase. Specifically, both the cubic and the hexagonal phases are found for the binary mixtures of the complex salt with water.

Another striking observation to be made from Figure 2 is that the classical associative phase separation, into one very dilute and one very concentrated phase, is restricted to rather narrow composition ranges on either side of the binary $C_{16}TAPA_{30}$/water axis. Phrased alternatively, a relatively small addition of either polyelectrolyte or surfactant to the complex salt suffices to ensure a complete miscibility with water. One can understand this as being an effect of the entropy of mixing of the numerous simple counterions that accompany the addition. The left phase diagram (Figure 2), the *polyion mixing plane*, refers to polyions with a mixture of surfactant micelles and simple monovalent ions as counterions. An increase in the fraction of monovalent counterions will, naturally, increase the solubility of this mixed salt. Conversely, in the right phase diagram (Figure 2b), the *surfactant ion mixing plane*, we find surfactant ions neutralized by a mixture of polyions and monovalent ions. Again, an increase in the fraction of the monovalent counterions increases the miscibility.

All our previous studies on the phase behavior of mixtures of alkyltrimethylammonium surfactants and polyacrylate, including those involving conventional polyelectrolyte/surfactant mixtures,[6,7] have been concerned with the specific combination of $C_{16}TA^+$ and PA_{30}^-. In the present study, we investigate the effects of changing the lengths of both the surfactant tail and the polyacrylate ion. Both these parameters may be suspected to influence the structures formed by the complex salt, its solubility in water, and the strength of the interaction between polyions and surfactant ions. Investigations from other laboratories have found a variation, with the surfactant chain length, of the structures separating out from conventional polyelectrolyte/surfactant mixtures,[9,11,12] including cross-linked polyelectrolytes.[15,16] In this study, we have produced and characterized the aqueous phase behavior of complex salts containing hexyl (C_6), octyl (C_8), decyl (C_{10}), dodecyl (C_{12}), or cetyl (C_{16}) trimethylammonium surfactants and polyacrylates of two different degrees of polymerization, that is, 30 and 6000. Most of the results pertain to binary complex salt/water mixtures, containing no simple ions. These binary mixtures correspond to the $C_{16}TAPA_{30}$/water axis in Figure 2.

Materials and Methods

Materials. Poly(acrylic) acids with nominal molar masses of 2000 (HPA_{30}) and 450 000 (HPA_{6000}) g/mol were purchased from Aldrich. A different batch of HPA_{30} from the same producer was previously examined by size-exclusion chromatography coupled with low-angle light scattering, giving a number-average molar mass $M_n = 2800$ g/mol and a weight-average molar mass $M_w = 4700$ g/mol.[7] Both polyacids were purified by dialysis for 5 days against Millipore water, followed by freeze-drying. ^{1}H NMR revealed a small amount of a structural impurity in the short polymer, which remained at unchanged intensity even after the dialysis procedure.[13] Two different batches of HPA_{30} both showed the presence of the impurity, which we ascribe to heterounits at the ends of the short polymer, originating from a termination reaction in the synthesis procedure. Titration of HPA_{30} with NaOH gave an equivalent molar mass of 89.3 g/(mol carboxylic acid), as compared with the theoretical value of 72 g/mol for a repeating unit of HPA. Presumably, this difference is due primarily to the heterounits in the polymer. Titration of the HPA_{6000} with NaOH gave an equivalent molar mass of 76.4 g/(mol carboxylic acid). The contribution from water to the equivalent molar masses should be small. The water uptake of the freeze-dried polyacids exposed to ambient air was found to be 2 wt % after 1 h and 5 wt % after several days. On the basis of the values of the equivalent molar masses, the number of repeating units is ~30 in HPA_{30} and ~6000 in HPA_{6000}.

The surfactants C_6TABr, C_8TABr, $C_{10}TABr$, and $C_{12}TABr$ were purchased from Tokyo Kogyo Co., Ltd. $C_{16}TABr$ was purchased from Merck. The surfactants were used without further purification.

Millipore water was used throughout the study.

Complex Salts. The complex salts were prepared by titrating the hydroxide forms of the surfactants with the polyacids, which is the same procedure that was used in our previous work.[13,14] The complex salts of this study will be named C_xTAPA_y, where x is the number of carbons in the surfactant chain and y is the number of repeating units in the polymer.

The first step of the synthesis was to convert C_xTABr into C_xTAOH by ion exchange.[17] The ion-exchange resin (Dowex SBR, dry mesh 20-50, from Sigma) was charged by stirring in an excess amount of 1 M NaOH for 2 h and then rinsed with Millipore water until the rinsing water reached pH 7. C_xTABr

TABLE 1: Aqueous Complex Salts as Obtained by Titration

complex salt C_xTAPA_y		pH at	
x	y	equivalence point	appearance
6	30	9.5	clear solution
8	30	9.4	clear solution
10	30	9.2	white precipitate
12	30	8.9	white precipitate
16	30	8.6	white precipitate
6	6000	10.3	clear solution
8	6000	10.0	clear solution
10	6000	9.6	white precipitate
12	6000	8.6	white precipitate
16	6000	8.2	white precipitate

(10−20 g) was then dissolved in a plastic beaker containing a large excess (100−200 g) of the charged ion-exchange resin and 100−200 mL of Millipore water. The solution was stirred for 2 h or, in the case of C_{16}TABr, until all was dissolved. The slurry was filtered, and the filtrate was rinsed with Millipore water into a fresh batch of 100−200 g of resin and 100−200 mL of water, which was stirred for another 2 h. The last step was repeated once. The alkaline solution now contained C_xTAOH at a concentration of approximately 0.05−0.075 M. Titrimetric analysis gave a bromide content below the detection limit of the analysis used (<0.1 wt % Br^-), demonstrating that the ion exchange was complete. The freshly prepared C_xTAOH solution was divided into two batches, to which 0.5 M solutions of HPA_{30} and HPA_{6000}, respectively, were added dropwise under stirring. This step was performed immediately to avoid Hofmann elimination of the quaternary ammonium hydroxide group of the surfactant in the basic solution.[18] The pH was measured using a standard KCl/AgCl pH electrode. The titration was continued until the pH of the equivalence point was reached in the solution; see Table 1. The equivalence point was taken as the inflection point from a separately determined pH titration curve. As is well-known, the polyacrylate ion is a stronger base than the acetate ion (see below) owing to the polyelectrolyte effect,[19] hence, the relatively high pH at the equivalence point (Table 1). The fact that the pH at the equivalence point decreases with increasing length of surfactant ion reflects a decreasing solubility of the corresponding complex salts.

The appearances of the solutions during titration differed. In most cases, a white precipitate was formed at the start of the titration. However, in the titration with the hexyl and octyl surfactant, the solutions remained clear and homogeneous; see Table 1. After equilibration overnight, the resulting systems (with precipitates or without) were freeze-dried. The complex salts were then obtained as white, hygroscopic powders or lumps, which were put to storage over silica gels in desiccators.

The surfactant cetyltrimethylammonium acetate C_{16}TAAc was prepared by the same procedure, that is, by titrating C_{16}TAOH with acetic acid, HAc, to the equivalence point (pH 8.1, as determined in a separate measurement). The resulting C_{16}TAAc solution was clear. After freeze-drying, C_{16}TAAc was obtained as a white powder and put to storage over silica gel in a desiccator.

Weighing experiments indicated that the water contents of the complex salts were 10 wt % for a salt stored in the desiccator and 20 wt % after prolonged storage in air. Care was taken to minimize the exposure of the components to air during sample preparation. A water content of 10 wt % in the complex salts was assumed when calculating the sample compositions.

Sample Preparation. Appropriate amounts of complex salt and water were weighed and put in glass tubes. The tubes were flame-sealed after mixing with a Vortex vibrator. Concentrated samples were mixed additionally in a centrifuge during 6 h at 4000 rpm and 40 °C, where the tubes were turned end over end every 15 min. The samples were left to equilibrate at 25 °C for several weeks.

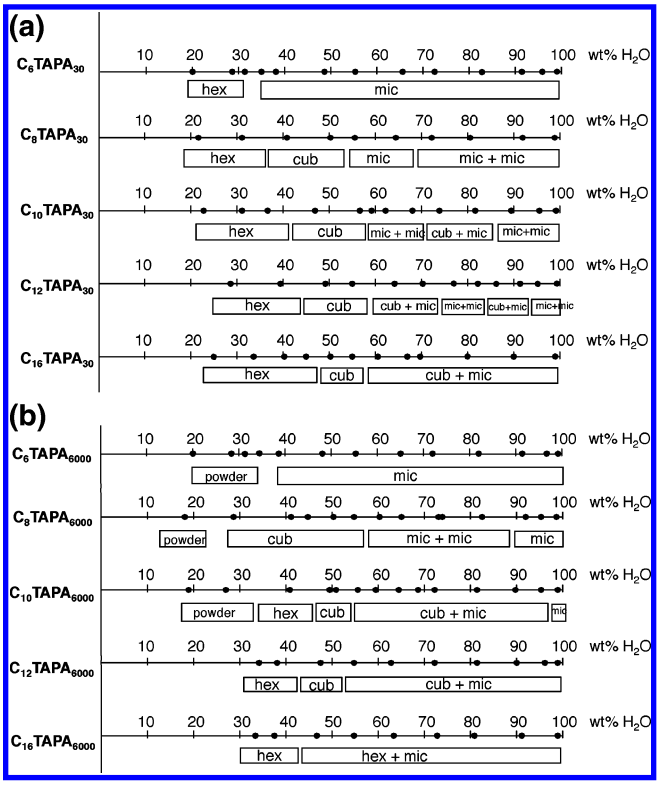

Figure 3. Phase sequences of binary mixtures of complex salts, C_x-$TAPA_y$, and water for varying surfactant chain lengths at 25 °C: (a) $y = 30$ and (b) $y = 6000$. The black dots indicate the composition of the investigated samples: "hex" = hexagonal phase, "cub" = cubic phase, and "mic" = micellar phase. Two-phase samples are denoted as, for example, "mic + mic".

Structures of Equilibrium Phases. All samples were investigated by visual inspection in normal light and between crossed polarizers to detect optically anisotropic phases (in the present case, the hexagonal phase). SAXS measurements were performed with a Kratky compact small-angle system with linear collimation. The X-rays were detected with a position sensitive detector. The wavelength was 1.54 Å, and the sample-to-detector distance was 277 mm. The sample cell had mica windows and was maintained at 25 °C.

Results

Figure 3 shows the phase sequences of the various complex salts at increasing water contents. The appearances of the samples varied, depending on the complex salt and the water content, from damp powders or hard, translucent samples at very low water contents to very dilute dispersions or clear solutions at very high water contents. At intermediate water contents, macroscopically phase-separated samples were found in most cases, containing one dilute liquid phase in equilibrium with either another clear liquid or a whitish solidlike phase. Cubic and/or hexagonal liquid crystalline phases were found for all complex salts except C_6TAPA_{6000}. The dry powders are beyond the scope of this study.

Below, we will first describe the phase behavior of the complex salts with the short polyion. Then we will give the corresponding result for the long polyions.

Short Polyion, Concentrated Region. All complex salts containing PA_{30} formed birefringent, stiff, and translucent

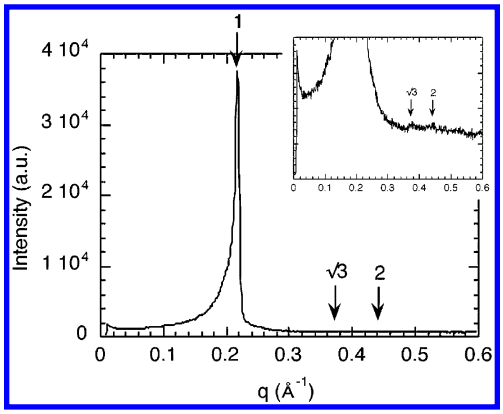

Figure 4. SAXS spectra of a hexagonal sample containing 69 wt % $C_{10}TAPA_{30}$ and 31 wt % water. The relative positions of the peaks correspond to a hexagonal structure.

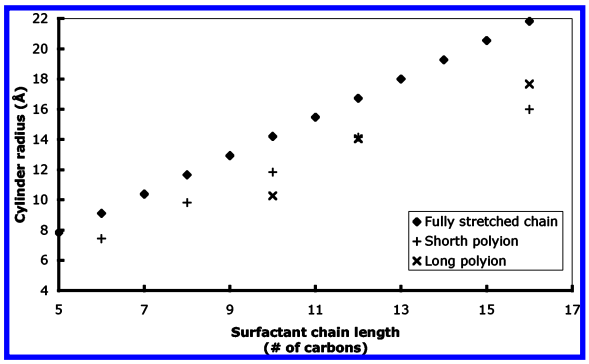

Figure 5. Hydrophobic core radii of C_xTAPA_y surfactant aggregates in the hexagonal phase for $y = 30$ (+) and 6000 (×). The diamonds (◆) show the lengths of fully stretched chains according to the equation $l = 0.15 + 0.127n_c$, where n_c is the amount of carbons in the surfactant chain.[20]

mixtures around 20 wt % water; see Figure 3a. SAXS measurements gave diffraction spectra with peaks at the relative positions 1, √3, and 2, showing that the samples were hexagonal. All hexagonal diffraction spectra in the study contained a strong first peak, followed by weak peaks at √3 and 2. An example is given in Figure 4, which shows the hexagonal SAXS spectrum of a $C_{10}TAPA_{30}$/water mixture.

The radius of the hydrophobic core of a hexagonal cylinder, containing surfactant alkyl chains only, was estimated according to

$$r = \sqrt{\frac{2\phi}{\pi\sqrt{3}}}\frac{2\pi}{q_1} \qquad (1)$$

where r is the radius, q_1 is the position of the first peak in the hexagonal spectrum, and ϕ is the volume fraction of surfactant alkyl chains in the sample. (ϕ was calculated by assuming a density of 1 g/mL both for the total sample and for the hydrophobic core of a cylinder.) Figure 5 shows the radius of the cylinder as a function of the number of carbons in the alkyl chain of the surfactant. The cylinder radius increases monotonically with increasing length of the alkyl surfactant chain. The calculated lengths of fully stretched alkyl chains are included in the figure for comparison.[20] The ratio between the cylinder radius and the length of the fully stretched chain varies between 0.72 and 0.85, implying that the alkyl chains in the cylinders are not fully stretched. This is expected; a ratio of 0.88 has previously been obtained for dodecyl chains in a hexagonal phase.[21]

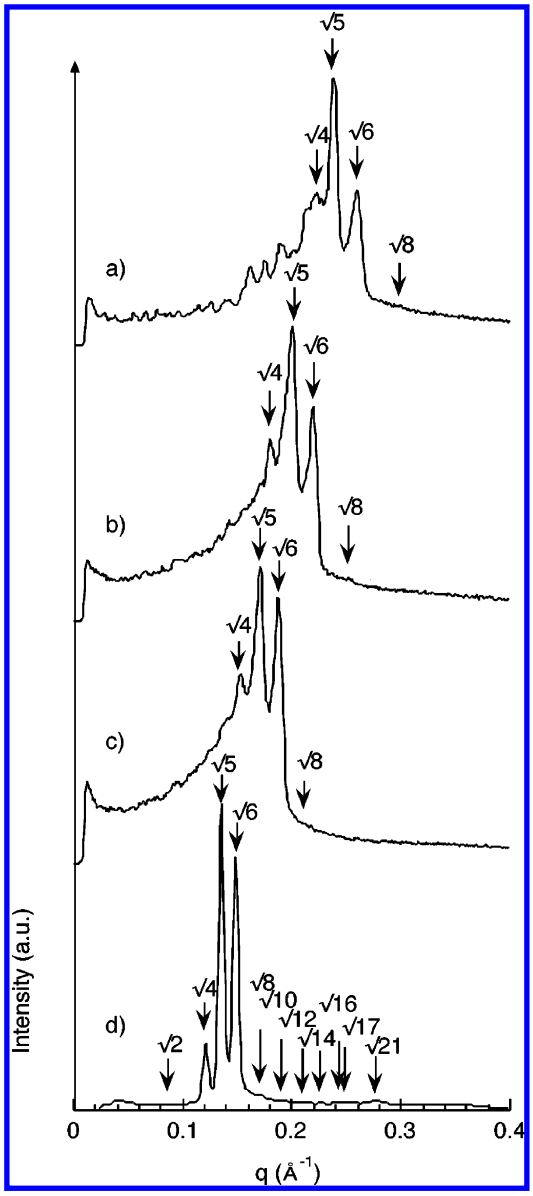

Figure 6. SAXS spectra of cubic phases in mixtures of complex salts with short polyion and water: (a) C_8TAPA_{30}/water, 50/50, (b) $C_{10}TAPA_{30}$/water, 43/57, (c) $C_{12}TAPA_{30}$/water, 45/55, and (d) $C_{16}TAPA_{30}$/water, 45/55 (ratios given in wt %). The relative positions of the peaks fit to the cubic *Pm*3*n* structure.

An increase in the water content to ca. 40−50 wt % water induced in most cases a phase transition from a birefringent to a nonbirefringent, hard, and transparent phase; see Figure 3a. C_6TAPA_{30} was an exception; here, a viscous, isotropic solution appeared at 34 wt % water. The SAXS spectra for the hard, transparent phase contained three characteristic large peaks with the relative positions √4, √5, and √6; see Figure 6. A small peak was also observed at √8, and in some cases, one was observed at √10. Thus, the spectra correspond to the micellar cubic phase *Pm*3*n*. The SAXS spectrum for $C_{16}TAPA_{30}$, Figure 6d, was performed by synchrotron X-ray diffraction in our previous study.[13] A well-resolved spectrum was obtained, and the *Pm*3*n* unit cell was identified with high accuracy (13 peaks fitted to the Miller indices). Hence, the diffraction pattern of the other complex salts can tentatively be ascribed to the same cubic unit cell, although only four or five peaks can be identified. In some spectra, additional small peaks, which did not match with the *Pm*3*n* Miller index, were found at low q values (before the √4 peak). The origin of these peaks is unknown.

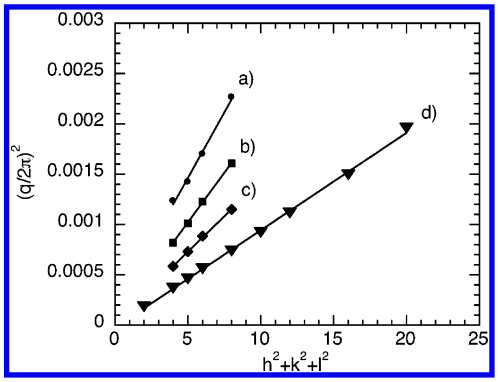

Figure 7. $(q/2\pi)^2$ from the SAXS spectra in Figure 6 vs the Miller index of the *Pm*3*n* unit cell. The slopes of the curves give the sizes of the unit cells, according to eq 2. The results are presented in Table 2.

TABLE 2: Unit Cell Dimensions and Micellar Aggregation Numbers for Cubic Samples of Aqueous Complex Salts

complex salt	water content (wt %)	unit cell size[a] (Å)	$N_{agg,theo}$[b]	N_{agg}[c]
C_8TAPA_{30}	50.0	61.7	27	34
$C_{10}TAPA_{30}$	56.7	73.3	40	44
$C_{12}TAPA_{30}$	55.0	84.2	56	64
$C_{16}TAPA_{30}$	55.3	101.6	95	100
C_8TAPA_{6000}	54.8	60.4	27	30
$C_{10}TAPA_{6000}$	55.5	70.5	40	42
$C_{12}TAPA_{6000}$	54.6	82.7	56	64

[a] Obtained by fits of eq 2 to the SAXS spectra in Figure 6. [b] Theoretical value for a spherical micelle of n_c carbon alkyl chains: $N_{agg,theo} = V_{hc}/\upsilon_{hc}$, where the volume of the micelle hydrocarbon core is $V_{hc} = 4\pi l_{hc}^3/3$, the length of a fully stretched hydrocarbon chain is $l_{hc} = 0.15 + 0.127n_c$, and the volume of a hydrocarbon chain is $\upsilon_{hc} = 0.027(n_c + n_{Me})$.[20] [c] Experimental value for the cubic samples, obtained as the number concentration of surfactant ions (assuming a density of 1 g/cm^3 for the samples) divided by the number concentration of micelles (obtained from the unit cell dimensions, with eight micelles per unit cell).

The size of the cubic unit cell, a, was obtained by plotting $(q/2\pi)^2$ vs the Miller indices of the *Pm*3*n* structure, according to

$$\left(\frac{q}{2\pi}\right)^2 = \left(\frac{1}{a}\right)^2 (h^2 + k^2 + l^2) \qquad (2)$$

Figure 7 shows fits of eq 2 to the SAXS spectra in Figure 6. The size of the cubic unit cell increases with increasing surfactant chain length; see Table 2. The unit cell size, together with the overall surfactant ion concentration, can be used to calculate the micellar aggregation numbers, N_{agg}, in the cubic phase. These values are given in Table 2 together with the corresponding theoretical predictions, $N_{agg,theo}$, for spherical micelles. The experimental values are 5−25% larger than the predicted values, consistent with the dominating view that the *Pm*3*n* cubic phase is a discrete micellar phase consisting of micelles that are only slightly aspherical.

The transition between the hexagonal and micellar cubic phases appears at different water contents depending on the surfactant chain length. C_8TAPA_{30} forms a cubic phase around 35 wt % water, whereas the transition appears at a higher water content, 47 wt % water, for $C_{16}TAPA_{30}$. Evidently, the stability of the hexagonal phase extends toward higher water contents with increasing surfactant chain lengths. The same trend is found in conventional surfactant systems, for example, octyltrimethylammoniumbromide has a phase transition from a hexagonal phase to a micellar phase at 28 wt % water,[21] whereas the same phase boundary appears at much higher water contents, 75 wt % water, for cetyltrimethylammoniumbromide.[22]

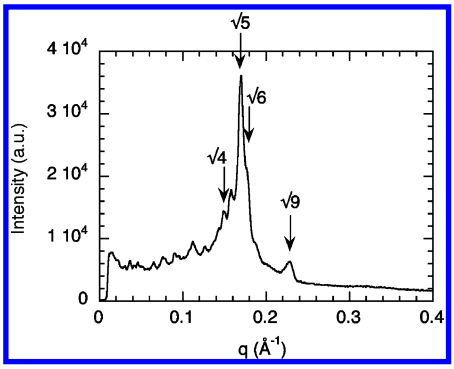

Figure 8. SAXS spectra of the concentrated phase in the two-phase region of $C_{12}TAPA_{30}$ at 71 wt % water. The relative positions of peaks are $q = 0.152$ Å^{-1} ($\sqrt{4}$), 0.171 ($\sqrt{5}$), 0.185 ($\sqrt{6}$), and 0.227 ($\sqrt{9}$).

The maximum swelling of the cubic phase is shifted slightly toward higher water contents as the surfactant chain length increases. The cubic phase ends at ca. 52 wt % water in the case of C_8TAPA_{30} and at ca. 55 wt % water for $C_{10}TAPA_{30}$, $C_{12}TAPA_{30}$, and $C_{16}TAPA_{30}$.

Short Polyion, Dilute Region. Above 55 wt % water, the complex salts in Figure 3a show a varying phase behavior. For the shortest surfactant chain, C_6TAPA_{30}, the micellar solution that appears at 34 wt % water extends as a single continuous phase all the way up to 100% water. For C_8TAPA_{30}, the stiff cubic phase is first transformed into a similar viscous micellar phase, but here, the concentrated micellar one-phase region is followed, at higher water contents, by a two-phase region with a concentrated micellar phase (bottom phase) in equilibrium with a dilute micellar phase (top phase).

The complex salt $C_{10}TAPA_{30}$ has a more complicated behavior. There is a micellar−micellar coexistence at 60 wt % water (two liquid phases on top of each other), which is transformed into a cubic phase (bottom phase) in equilibrium with a micellar phase (top phase) at 70 wt % water. At 90 wt % water, the two micellar phases reappear. Finally, at 99 wt % water, the (small) concentrated phase is again solidlike. This puzzling behavior, which violates the Gibbs phase rule for a two-component system, will be discussed further below.

The complex salt with dodecyl chains ($C_{12}TAPA_{30}$) displays a similarly complicated phase behavior above 55 wt % water, showing sometimes micellar−micellar and sometimes cubic−micellar coexistence. Here, a density inversion has taken place and the concentrated phase is now the top phase of a phase-separated sample. The cubic phase from biphasic samples in the dilute region gave SAXS spectra that poorly fit to the *Pm*3*n* unit cell for the $C_{12}TAPA_{30}$ case; see Figure 8. Similar spectra were obtained in some instances also for biphasic samples of $C_{12}TAPA_{6000}$. Repeat measurements with samples from a new batch of $C_{12}TA^+$ gave normal *Pm*3*n* spectra for $C_{12}TAPA_{6000}$ but not for $C_{12}TAPA_{30}$. At present, we do not understand the origin of this anomalous spectrum, but it could represent a poorly equilibrated sample.

The complex salt with cetyl chains, finally, shows a more straightforward phase sequence, which has been described in detail in previous publications.[13,14] The cubic phase swells up to 55 wt % water and is then followed by a two-phase region at increasing water contents, where a cubic *Pm*3*n* top phase is in equilibrium with a dilute bottom phase. The onset of phase separation is difficult to detect due to the stiffness of the cubic phase, which gives rise to an entrapment of domains of the dilute phase inside the concentrated phase. This feature was discussed

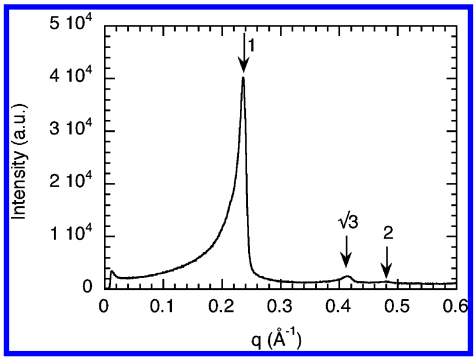

Figure 9. SAXS spectra of a hexagonal sample containing 59 wt % $C_{10}TAPA_{6000}$ and 41 wt % water. The relative positions of the peaks correspond to a hexagonal structure.

earlier.[13,14] As the dispersion gives rise to light scattering, the samples acquire an opaque texture. Upon further dilution, a macroscopic phase separation eventually appears, with a clear dilute phase in addition to the opaque dispersion. The phase boundary was taken as the point where the turbidity of the cubic phases started to increase noticeably.

Long Polyion, Concentrated Region. The same liquid crystalline structures were found for the complex salts with the long polyion; see Figure 3b. However, the samples were more difficult to homogenize, which was attributed to the slower molecular diffusion of the long polymer. Most of the samples obtained a whitish texture at first, where the turbidity disappeared gradually after a couple of months.

The hexagonal phase appears at ca. 30 wt % water for the complex salts containing decyl, dodecyl, and cetyl chains. The SAXS spectrum of a hexagonal sample of aqueous $C_{10}TAPA_{6000}$ is shown in Figure 9. We did not find any hexagonal phase for the complex salts with octyl or hexyl chains.

The radius of the hexagonal cylinder was calculated in the same way as that for the salts of the short polyion, but the absence of homogeneous hexagonal phases with the octyl and hexyl chain surfactants limits the data set. It appears nonetheless that the cylinder radius increases with the number of carbons in the surfactant alkyl chain; see Figure 5.

The cubic phase was found in the phase sequence of the complex salts with octyl, decyl, and dodecyl chains. The extension of the cubic phase region is largest for C_8TAPA_{6000}, covering water contents from 29 to ca. 57 wt % water. For $C_{10}TAPA_{6000}$ and $C_{12}TAPA_{6000}$, the cubic phase appears at ca. 45 wt % water. The maximum swelling of the cubic phase (i.e., the phase boundary at high water contents) is at ca. 57 wt % for C_8TAPA_{6000} and decreases slightly for decyl and dodecyl chains. The SAXS spectra of the monophasic cubic samples (not shown) were quite similar to those obtained for the cubic samples of the complex salts with the short polyion; see Figure 6. The sizes of the cubic unit cells, obtained by fits to eq 2, as well as the micellar aggregation numbers, were also similar to the corresponding data for the complex salts with the short polyion; see Table 2.

The cubic phase did not appear for the complex salts with hexyl and cetyl chains. No liquid crystalline phases were found with hexyl chains, and the phase sequence of C_6TAPA_{6000} contains a large micellar phase above 35 wt % water. For the complex salt with cetyl chains, the hexagonal phase borders to a wide two-phase area, where the hexagonal phase is in equilibrium with a dilute aqueous phase. To check whether the absence of the cubic phase could be due to a slow development of the equilibrium structure, a biphasic sample of the complex salt with cetyl chains was prepared by another route. $C_{16}TAPA_{6000}$ was dissolved in water through the addition of 0.5 M of a simple salt, $NaNO_3$. (Salt screens the electrostatic attraction between the polyions and the surfactant aggregates, resulting in a dissolution.) The homogeneous solution was then poured into a dialysis bag, which was subsequently dialyzed against a large reservoir of Millipore water. The water was replaced every day during one week. As the concentration of the simple salt decreased inside the bag, the screening gradually disappeared and the polyion−surfactant ion complex salt reprecipitated from the homogeneous solution. SAXS measurements of the precipitate revealed a hexagonal structure. Hence, it was concluded that the structure of aqueous $C_{16}TAPA_{6000}$ that is in equilibrium with excess water is indeed the hexagonal phase.

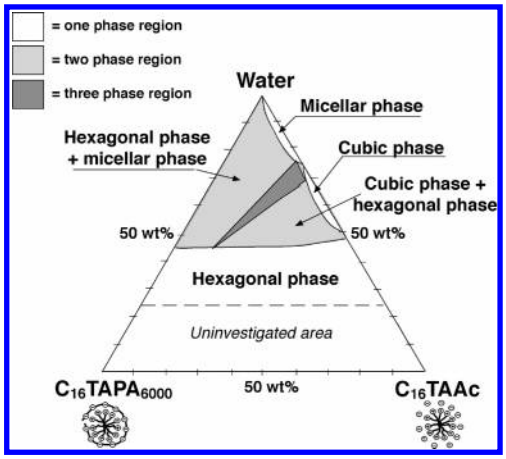

Figure 10. Experimental phase diagram of the complex salt $C_{16}TAPA_{6000}$, the surfactant $C_{16}TAAc$, and water at 25°C.

To further investigate the effect of the long polyion on the cubic *Pm*3*n* phase, ternary mixtures were made of the complex salt $C_{16}TAPA_{6000}$, the surfactant $C_{16}TAAc$, and water. The phase diagram is presented in Figure 10 and may be compared with the corresponding surfactant ion mixing plane for the short polyion, as shown in Figure 2. It is evident that a large part of the phase diagram for the long polyion is covered by a two-phase region, where the hexagonal phase is in equilibrium with a micellar phase. The cubic region at the $C_{16}TAAc$/water axis disappears at small contents of $C_{16}TAPA_{6000}$, showing that the cubic phase can hardly incorporate any polyion. The phase diagram clearly shows that the long polyion favors a hexagonal packing of the cetyl surfactant aggregates.

Long Polyion, Dilute Region. Above 55 wt % water, all complex salts with the long polyion, except C_6TAPA_{6000}, were biphasic, with a concentrated phase in equilibrium with a dilute phase; see Figure 3b. For octyl chains, the concentrated phase gave rise to a single broad peak, indicating a disordered micellar phase, in the SAXS experiment; see Figure 11. The concentrated phase with decyl and dodecyl chains had a cubic *Pm*3*n* structure, as evidenced by spectra similar to those shown in Figure 6. The complex salt with cetyl chains formed a hexagonal structure in the concentrated phase, as explained above.

A density inversion occurred with increasing surfactant chain length, as in the complex salts with the short polyion. The cubic phases were heavier than the dilute phases for C_6TAPA_{6000}, C_8TAPA_{6000}, and $C_{10}TAPA_{6000}$, whereas the concentrated phases of $C_{12}TAPA_{6000}$ and $C_{16}TAPA_{6000}$ were lighter than water and hence appeared as the top phases in the tubes. The density inversion shows that 1 g/cm^3 is a valid approximation for the overall density in the systems.

Effect of Polyion Length in NaPA/C_{16}TABr Mixtures. To further elucidate the effect of the polyion length on the liquid

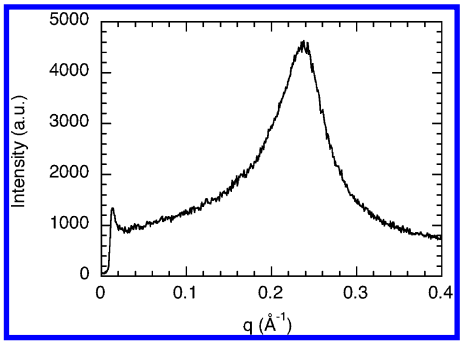

Figure 11. SAXS spectrum of the concentrated phase in the two-phase region of C_8TAPA_{6000} at 73 wt % water.

TABLE 3: Structures of the Complex Salts Obtained from Mixing 0.005 M NaPA (in terms of charges) and 0.005 M $C_{12}TABr$ or $C_{16}TABr$

MW PA g/mol	structure of $C_{12}TABr$ + NaPA	structure of $C_{16}TABr$ + NaPA
2000	cubic	cubic
5000		cubic
20 000		hexagonal
60 000		hexagonal
140 000		hexagonal
250 000		hexagonal
450 000	cubic	hexagonal

crystalline structures, mixtures of NaPA and $C_{16}TABr$ were made for a series of polyacrylate samples with different molecular weights; see Table 3. The aim was to find out at what chain length the change occurs from a cubic to a hexagonal structure in equilibrium with excess water. Equivalent amounts (in terms of charge) of NaPA and $C_{16}TABr$ were mixed at low concentrations (5 mM). The phase separation in dilute mixtures of NaPA and $C_{16}TABr$ has previously been shown to give a concentrated phase containing mostly $C_{16}TA^+$ and PA^- (i.e., the complex salt), in equilibrium with a dilute phase containing essentially only Na^+ and Br^- ions.[7] SAXS measurements were made on the precipitates obtained from the various NaPA + $C_{16}TABr$ mixtures, and the structures obtained are listed in Table 3. Polyacrylate with molar masses of 2000 and 5000 g/mol gave cubic structures, whereas molar masses of 20 000 g/mol and higher gave hexagonal structures. Hence, the change in structure of the complex salt $C_{16}TAPA_y$ seems to appear at a molar mass below 20 000 g/mol. In this context, we note that cubic structures have also been reported in mixtures of cetylpyridinium surfactants and NaPA with the molar mass 10 000 g/mol.[11]

Similar dilute mixtures of the dodecyl surfactant $C_{12}TABr$ with $NaPA_{30}$ and $NaPA_{6000}$ both gave precipitates with cubic structures (see Table 3) in accordance with the phase behavior of the corresponding complex salts ($C_{12}TAPA_{30}$ and $C_{12}TAPA_{6000}$; see Figure 3b).

Solubility. The extension of the micellar phase regions in the phase sequences in Figure 3 shows that the solubility of the complex salts decreases with increasing length of the surfactant chains. The complex salts with hexyl chains form large micellar phase regions, that is, are totally soluble, whereas complex salts with longer surfactant chain length give rise to phase-separated samples. Surprisingly, the reverse trend is implied by our results for the polyion: the dilute micellar phase extends to higher complex salt concentrations, indicating a higher water solubility, for the long polyion in the salts with the octyl and decyl chain surfactants. This result will be followed up in a detailed investigation of the very dilute region of the phase diagrams, which is currently underway in our laboratory.

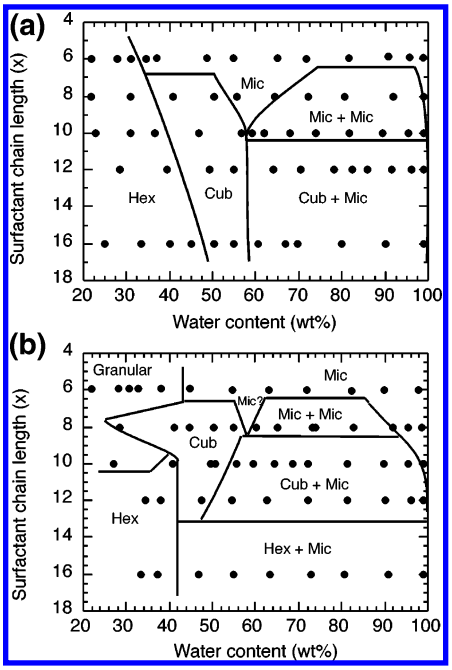

Figure 12. Global phase diagrams of C_xTAPA_y/water mixtures drawn to illustrate the effect of the surfactant chain length: (a) C_xTAPA_{30} (top) and (b) C_xTAPA_{6000} (bottom).

Discussion

Global Phase Diagrams. The primary objective of the present work is to investigate and understand the effects of surfactant chain length and polyion length on the structure and maximum water uptake of complex surfactant ion/polyion salts immersed in water. For the purpose of our further discussion, we summarize, in Figure 12, the global trends in Figure 3 in two diagrams, with the water content and the surfactant chain length as the variables. The plotted diagrams are not true phase diagrams, since the surfactant chain length is not a continuous variable; each step along the *y*-axis thus corresponds to a change of system. Still, we argue that the diagrams provide a useful basis for a deeper molecular understanding.

We first note that especially the diagram in Figure 12a has many features in common with the temperature−density phase diagram for a simple atomic fluid,[23] or with a phase diagram for attractive colloidal spheres in a solvent,[24] with the strength of the attraction decreasing along the *y* axis. If we, in Figure 12, only consider the phases containing small micelles, we can identify a concentrated "solid" region, where the micelles crystallize in a cubic phase, as well as a "fluid" phase of disordered micelles, with a concentrated "liquid" and a dilute "gas" branch. The liquid phase only appears for short surfactant chains, in the top parts of the phase diagrams. We have recently shown that the phase diagram in Figure 2b, representing mixtures of $C_{16}TAPA_{30}$ and $C_{16}TAAc$ in water, can be plotted in a similar fashion, where the proportion of polymeric counterions is the variable that controls the interaction strength between the micellar aggregates.

Effects of Surfactant Chain Length. The overall effect of decreasing the surfactant chain length (Figure 12) is to increase the miscibility between the complex salt and water. How do we understand this trend in terms of the interactions in the system? We believe that the dominating effect is an increasing fraction of monomeric (nonmicellized) surfactant ions. In general, we can view our complex salts as being composed of polyions, neutralized by a mixture of micellar aggregates and free monomeric surfactant ions. The proportion of monomeric

surfactant ions is very small for C_{16}TAPA (10^{-4} in the cubic phase, according to our recent studies by NMR self-diffusion[25]) but should be much higher for the shortest surfactant chains of our study. The general effect of increasing the fraction of monomeric counterions to the polyions, at the expense of the micelles, is illustrated in Figure 2a, the phase diagram of mixtures of $NaPA_{30}$ and $C_{16}TAPA_{30}$ in water, which shows that an increasing fraction of small counterions in the system increases the solubility of the complexes.

Another factor that should contribute to the increased miscibility with water is the decreased size of the micelles. As the micelle size is decreased, the number of micelles increases. Consequently, the entropy of mixing of the micelles increases and the interaction strength per micelle decreases. The decrease in micelle size may also affect the packing of the micelles and polyions. Efficient packing requires that the polyion is sufficiently flexible enough to be able to wrap around the micelles,[26,27] a condition that becomes increasingly difficult to fulfill as the micelles become smaller.

At this stage, we cannot evaluate the quantitative importance of the two effects discussed above, that is, the increase in the fraction of monomeric surfactant ions and the decrease in micellar size. Further measurements, by NMR self-diffusion[25] of the fraction of monomeric surfactant ions in the various cubic phases, should clarify this point.

Figure 12 also allows us to evaluate the variation, with surfactant chain length, in the structures of those concentrated phases that are at equilibrium with the dilute phases in water-rich samples. These should closely correspond to the structures that separate out from conventional mixtures of C_xTABr and NaPA at high dilution.[6] When moving from C_{16} to C_6 surfactant chains, the sequence for the long polyion is hexagonal−cubic *Pm*3*n*−micellar. Similar sequences have been found for the concentrated phases separating out from conventional 1:1 mixtures of cationic starch and anionic surfactant, where changing from C_{16} to C_{10} chains gave a phase sequence of hexagonal−HCP (spherical micelles in a hexagonal packing)−micellar.[12] Figure 12 allows us to obtain a deeper insight in the origin of such a sequence. It appears that the major reason for the variation in the structures is that the concentrated phase that separates out becomes less concentrated (more water-rich) as the surfactant chain length decreases. The variation in structure is much weaker if the concentrated phases are compared at the same water content, that is, along the vertical lines in Figure 12.

Effects of Polyion Length. Our study has revealed quite a strong effect on the phase behavior of increasing the polyion chain length beyond 30 repeating units. The effect is clearly seen by comparing parts a and b of Figure 12 and, also, the phase diagrams in Figure 2b and Figure 10, respectively. Both comparisons show that a large increase in the polyion length gives rise to a strong increase in the miscibility gap with water. While a polyion length dependence in general must exist, a leveling off beyond some finite length may also be expected. Extensive Monte Carlo simulations of the interactions between charged surfaces neutralized by polymeric counterions have indicated that the effects of the polyion length are small already beyond a few repeating units.[28] In view of the latter findings, our results are far from obvious. Table 3 indicates that a significant polyion length dependence of the phase behavior persists at least to lengths of the order of 10^2 repeating units for C_{16} chains.

Figure 12 indicates that an increase in the polyion length increases the attraction between polyions and the surfactant aggregates. This is shown by the fact that the maximum water content of the concentrated phase, at the boundary to the wide biphasic area, is always lower for the longer polyion, at a given surfactant chain length. Hence, the concentrated phase becomes more concentrated with the long polyion. This effect provides an explanation for the disappearance of the cubic phase for long surfactant chains and long polyions. A high surfactant concentration favors a hexagonal packing. The results in Figure 12b thus suggest that, for long surfactant chains, the interactions with the long polyion are sufficiently strong enough to produce concentrations where the hexagonal structure is the most favorable packing of the surfactant aggregates. This interpretation further suggests that the cubic phase may appear upon addition of small amounts of excess simple salt, since salt screens the attraction.

Irregularities in the Phase Sequences. In the schematic diagrams in Figure 12, we have neglected the complicated phase sequences obtained in the wide biphasic areas for some of the mixtures in Figure 3: For both $C_{10}TAPA_{30}$ and C_8TAPA_{6000}, the monophasic cubic samples were followed by samples showing micellar−micellar (rather than cubic−micellar) coexistence, upon increasing the water content. Moreover, $C_{10}TAPA_{30}$ and $C_{12}TAPA_{30}$ displayed puzzling "oscillations" between cubic−micellar and micellar−micellar coexistence in the wide biphasic area. These features indicate that, in all of these mixtures, the free energy difference between a concentrated micellar phase and a cubic phase is small. Figure 12 supports this notion; all of the "problematic" mixtures are situated close to a line that separates the micellar−micellar coexistence from cubic−micellar coexistence. Small perturbations in the system, presumably due to the polydispersity of the polyion component, may then suffice to shift the equilibrium across the line.

Conclusions

The investigated set of complex salts, involving five different surfactant chain lengths and two polyion lengths, has been shown to conform to a consistent picture, represented by the global phase diagrams in Figure 12. Aqueous mixtures of these complex salts feature the same phases, that is, hexagonal, cubic *Pm*3*n*, and micellar, as have previously been found in polyion−surfactant mixtures based on the C_{16} surfactant and a short polyacrylate (30 repeating units).

The attraction between polyions and surfactant aggregates, as manifested in the miscibility of the complex salts with water, increases both with increasing surfactant chain length and with increasing polyion length. The complex salts with the shortest surfactant (C_6) are completely miscible with water; all of the others display a miscibility gap with water. For the latter, the structure of the concentrated phase (hexagonal, cubic, or micellar) that exists at the maximum degree of swelling, that is, in equilibrium with excess water, seems to mainly depend on the water content which, in turn, is determined by the strength of the attraction. A weak attraction (short polyions, short surfactant chains) results in a salt that can take up a lot water and thus swells all the way to the disordered micellar structure. By contrast, a sufficiently strong attraction (long polyions, long surfactant chains) results in a salt that does not swell beyond the hexagonal phase.

Acknowledgment. This study was funded by the Swedish National Graduate School of Colloid and Interface Technology (A.S.) and the Swedish Research Council (L.P.).

References and Notes

(1) Goddard, E. D. *Colloids Surf.* **1986**, *19*, 301.

(2) Kwak, J. C. T. *Polymer-surfactant systems*; Marcel Dekker: New York, 1998.
(3) Thalberg, K.; Lindman, B. Polymer-surfactant interactions—recent developments. In *Interactions of surfactants with polymers and proteins*; Goddard, E. D., Ananthapadmanabhan, K. P., Eds.; CRC Press: Boca Raton, FL, 1993; p 203.
(4) Piculell, L.; Lindman, B. *Adv. Colloid Interface Sci.* **1992**, *41*, 149.
(5) Piculell, L.; Lindman, B.; Karlström, G. Phase behaviour of polymer/surfactant systems. In *Polymer-surfactant systems*; Kwak, J. C. T., Ed.; Marcel Dekker: New York, 1998; Vol. 77.
(6) Ilekti, P.; Martin, T.; Cabane, B.; Piculell, L. *J. Phys. Chem. B* **1999**, *103*, 9831.
(7) Ilekti, P.; Piculell, L.; Tournilhac, F.; Cabane, B. *J. Phys. Chem. B* **1997**, *102*, 344.
(8) Antonietti, M.; Conrad, J. *Angew. Chem., Int. Ed. Engl.* **1994**, *33*, 1869.
(9) Antonietti, M.; Conrad, J.; Thunemann, A. *Macromolecules* **1994**, *27*, 6007.
(10) Zhou, S.; Yeh, F.; Burger, C.; Chu, B. *J. Phys. Chem. B* **1999**, *103*, 2107.
(11) Kogej, K.; Evmeneko, G.; Theunissen, E.; Berghmans, H.; Reynaers, H. *Langmuir* **2001**, *17*, 3175.
(12) Merta, J.; Torkkeli, M.; Ikonen, T.; Serimaa, R.; Steniua, P. *Macromolecules* **2001**, *34*, 2937.
(13) Svensson, A.; Piculell, L.; Cabane, B.; Ilekti, P. *J. Phys. Chem. B* **2002**, *106*, 1013.
(14) Svensson, A.; Piculell, L.; Karlsson, L.; Cabane, B.; Jönsson, B. *J. Phys. Chem. B* **2003**, *107*, 8119.
(15) Khandurina, Y. V.; Dembo, A. T.; Rogacheva, V. B.; Zezin, A. B.; Kabanov, V. A. *Polym. Sci.* **1994**, *36*, 189.
(16) Zhou, S.; Burger, C.; Yeh, F.; Chu, B. *Macromolecules* **1998**, *31*, 8157.
(17) Nydén, M.; Söderman, O. *Langmuir* **1995**, *11*, 1537.
(18) Morrison, R. T.; Boyd, R. N. *Organic Chemistry*, 4th ed.; Allyn and Bacon Inc.: Newton, MA, 1983.
(19) Mandel, M. *Eur. Polym. J.* **1970**, *6*, 807.
(20) Evans, D. F.; Wennerström, H. *The colloidal domain—where physics, chemistry, biology and technology meet*, 2nd ed.; John Wiley & Sons: New York, 1999.
(21) Fukada, K.; Matsuzaka, Y.; Fujii, M.; Kato, T.; Seimiya, T. *Thermodyn. Acta* **1998**, *308*, 159.
(22) Wärnheim, T.; Jönsson, A. *J. Colloid Interface Sci.* **1988**, *125*, 627.
(23) Vliegenthart, G. A.; Lodge, J. F. M.; Lekkerkerker, H. N. W. *Physica A* **1999**, *263*, 378.
(24) Lekkerkerker, H. N. W. *Physica A* **1997**, *244*, 227.
(25) Svensson, A.; Topgaard, D.; Piculell, L.; Söderman, O. *J. Phys. Chem. B* **2003**, *107*, 13241.
(26) Jonsson, M.; Linse, P. *J. Chem. Phys.* **2001**, *115*, 10975.
(27) Skepö, M.; Linse, P. *Macromolecules* **2003**, *36*, 508.
(28) Woodward, C. E.; Jönsson, B.; Åkesson, T. *J. Chem. Phys.* **1988**, *89*, 5145.